Colloid Polym Sci (2003) 282: 41–47
DOI 10.1007/s00396-003-0908-z

ORIGINAL CONTRIBUTION

Galo Cárdenas
Silvana Salinas
Ricardo Oliva

Synthesis and characterization of palladium–tin bicolloids prepared by chemical liquid deposition

Received: 23 September 2002
Accepted: 12 March 2003

G. Cárdenas (✉) · S. Salinas · R. Oliva
Departamento de Polímeros,
Facultad de Ciencias Químicas,
Universidad de Concepción,
Casilla 160-C, Concepción, Chile
E-mail: gcardena@udec.cl

Abstract Palladium–tin bicolloids have been prepared by chemical liquid deposition. The metals were cocondensed at 77 K with ethanol, 2-propanol, 2-methoxyethanol, 2-butanone and acetone. The distribution of particle sizes was determined by transmission electron microscopy of the stables dispersions. The sizes ranged from 3.8 nm for 2-methoxyethanol to 8.3 nm for acetone colloids. Electrophoretic measurements such as colloid charge and zeta potential were achieved. It was found that the colloids possess electrical charge; therefore, it is postulated that their stability is by simple solvatation. The colloids showed stability over 1 week at room temperature. The zeta-potential values are in agreement with the stability and electrophoretic mobility. The highest zeta potential was obtained for PdSn–2-methoxyethanol colloids with 379 mV and the lowest for 2-butanone with 114 mV. The colloids exhibit absorption bands in the UV region. In the visible region no plasma absorption was found. Active solids obtained by evaporation of the solvent contain a certain amount of the solvent incorporated, and owing to their reactivity they produce a mixture of tin oxide with palladium and tin. The presence of solvents can be observed by Fourier transform IR incorporation in the finely divided solids. Characteristic bands for each solvent were measured. By means of thermogravimetric analysis and differential scanning calorimetry the thermal stability of the solids and the transition heat give us the carbonaceous residues in the films. The elemental analysis of the powders was carried out.

Keywords Nanostructures · Colloids · Infrared microscopy · Vapor deposition · Electron microscopy

Introduction

The use of cocondensation of metal atoms with organic solvents at 77 K is a known technique and provides several reactions [1]. Solvated metal atoms seem to be associated with weakly stabilized colloidal dispersions; the improvement of this solvation process has been shown to be a precursor for new metallic colloids [2,3], some of them very stable at room temperature, like palladium and gold [4,5]. In fact, during the past few years [6, 7, 8] some general approaches of broad applicability in preparing highly active metal aggregates with nanometric sizes have been achieved. Several techniques have been developed for the preparation of nanoparticles with semiconducting properties.

The synthesis and processing of nanostructured materials have been reviewed by different authors

[9,10,11]. Our approach has been the solvated metal atom dispersion method with nonaqueous solvents [8]. In this way, nanocolloidal metallic dispersion can be obtained. By direct evaporation under vacuum, we have been able to obtain a variety of metallic films and active solids with nanoclustered structures [12,13]. The most successful approaches for the preparation of stable metal colloids in organic solvents are based on the clustering of metal atoms at low temperature [14].

Optically functional materials were prepared by dispersing semiconductor nanoparticles into films, glass or ceramic matrices. These materials are electrodes for the study of the linear and nonlinear optical properties of nanoparticles, including absorption, fluorescence and other optical nonlinearity [15,16]. Greater optical nonlinearities can be obtained in PbS nanoparticle dispersed films [17].

This paper examines the correlation between stabilities and particle size of colloids and also with aging for Pd–Sn bimetal colloids. The UV absorption of the colloids was measured. Finally, a complete study by IR and thermogravimetric analysis (TGA)-Fourier transform (FT) IR spectroscopy was carried out to determine the solid composition.

Experimental

Preparation of metal colloids

The bimetal atom reactor has been recently described [13,14]; as a typical example, alumina–tungsten crucibles were charged separately. Pd metal (pieces) and Sn metal (lumps) were used. Dry acetone was placed in a ligand inlet tube and freeze–pump–thaw degassed with several cycles. The reactor was pumped down to 0.008 mbar while the crucible was warmed to red heat. A liquid-nitrogen-filled Dewar flask was placed around the vessel and Pd with Sn and acetone (52 ml) were deposited over 1 h using 40 and 30 A, respectively. The matrix was a blue/purple color at the end of the deposition. The matrix was allowed to warm slowly under vacuum by removal of the liquid-nitrogen-filled Dewar flask for 1 h; upon meltdown a brown colloid was obtained. After addition of nitrogen up to 1 atm, the colloid was allowed to warm for another 0.5 h at room temperature. The solution was siphoned out under nitrogen into a flask. On the basis of the amount of metal evaporated and acetone allowed in the molarity in terms of metal could be calculated. Solutions of several concentrations were prepared under the same conditions.

The film was obtained by stripping the solvent under vacuum. The solvent evaporation on a substrate can be speeded by a N_2 flow or by using a warm substrate.

Electron microscopy studies

Transmission electron micrographs were obtained using a JEOL JEM 1200 EX II with 4-Å resolution by using copper grids coated with carbon foil. A drop of the colloid was placed on a copper grid and allowed to dry.

Thermogravimetric analysis

A PerkinElmer model TGA-7 thermogravimetric system, with a microprocessor-driven temperature control unit and TA data station was used. The sample weight was recorded and generally ranged between 5 and 10 mg. The sample was placed in the balance system and the temperature was raised from 25 to 550 °C at a heating rate of 10 °C min^{-1}. The sample weight was continuously recorded as a function of temperature.

IR studies

IR spectra were obtained using a Nicolet 5PC spectrometer. KBr pellets were made for all the films at 2% concentration. Spectra were recorded at a resolution of 2 cm^{-1} and a minimum of 128 scans were accumulated.

UV–vis spectroscopy

A PerkinElmer 2100 spectrophotometer was used. The solvent was employed as a reference; the sample spectra between 200 and 800 nm were recorded.

Zeta potential

A Laser Zee meter model 501, Pen Kem, was used. The charge and zeta potential of the colloid were measured.

Thermogravimetric analysis–Fourier transform IR spectroscopy

Experiments were performed using a Nicolet Magna 550 system consisting of a FTIR spectrophotometer with a detector coupled to a PerkinElmer TGA-7. TGA sample weights in these studies ranged from 8 to 10 mg. Under a nitrogen purge, a heating rate of 10 °C min^{-1} was used to scan from 25 to 550 °C. The heated line which transferred the evolved gases from the TGA-7 system to the FTIR spectrometer was maintained at 240 °C.

Results and discussion

Palladium–tin bicolloids were obtained by cocondensation of the metal with several solvents such as ethanol, 2-propanol, 2-methoxyethanol, 2-butanone and acetone.

The stability of the colloid was defined as the time that metal particles remain as sols at room temperature. Systems such as Pd–Sn in ethanol are stable for weeks; in 2-propanol the stability increases to 3 weeks.

There is a compromise between the dielectric constant and the viscosity. In alcohols, the higher viscosity helps to solvate the metal clusters much better. On the other hand, acetone is more stable at low colloid concentration than 2-butanone, but in this case their viscosities are similar and acetone is comparable to 2-methoxyethanol colloids [18].

The following scheme summarizes the synthesis of the bimetallic colloids and active solids.

$$\mathrm{Pd_{atoms}+Sn_{atoms}+solv.} \xrightarrow[\text{77 K}]{\text{Cocondensation}} \mathrm{Pd-Sn solv.\ matrix}$$

Warmup ↓ Meltdown

$$\mathrm{(Pd)_n-(Sn)_m solv. slurry} \leftarrow \mathrm{(Pd-Sn) solution/dispersion}$$

Blue/purple
↓
Pd – Snfilm/powder
(brown)

The higher stability of 2-methoxyethanol (around 2 months) colloids is mainly because they can produce five- or six-membered rings, which are thermodynamically very stable (Structures 1 and 2).

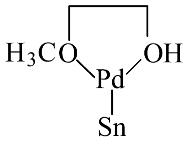

1

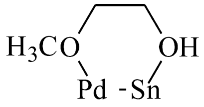

2

An important feature of these colloids is that most are negatively charged; this is very similar to previous reports [19,20]. The charge comes form the pyrolisis of a small amount of solvent on the hot metal vaporization source or is due to reactions between ketones and metal atoms. For that reason their migration velocity is higher than the other solvents.

The higher zeta potential found for the (PdSn)–2-methoxyethanol (379 mV) colloid is indicative of greater stability; this is followed by the bimetallic (PdSn)–acetone (153 mV) colloid, which exhibits a

Table 1 Stability, particle size and zeta potential of Pd–Sn colloids

Solvent	Concentration (mol $l^{-1}\times10^{-3}$)	Color	Stability (days)	Particle size (nm)	μ_E ($m^2\ V^{-1}\ s^{-1}\times10^{-9}$)
2-Propanol	0.231	Light brown	30	5.8	
	1.13	Brown	> 21	–	
	2.24	Dark brown	21	–	2.14
	3.78	Dark brown	21	–	
Ethanol	0.229	Light brown	21	5.7	
	1.11	Brown	> 14	–	
	2.33	Dark brown	> 14	–	6.61
	3.61	Dark brown	> 14	–	
2-Methoxyethanol	2.32	Dark brown	> 49	3.8	8.75
	3.71	Dark brown	> 49	–	
Acetone	0.228	Light brown	> 56	8.3	
	1.13	Brown	> 56	–	
	2.36	Dark brown	28	–	10.41
	3.34	Dark brown	21	–	
2-Butanone	2.28	Dark brown	> 30	5.9	10.38
	4.04	Dark brown	> 21	–	

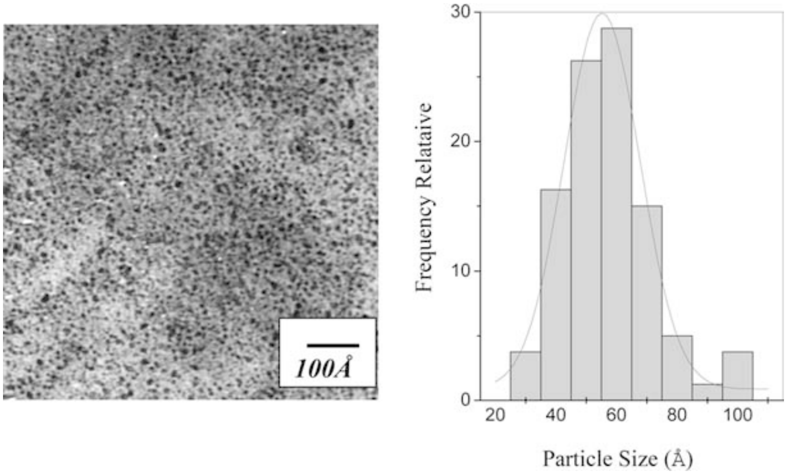

Fig. 1 Electron micrograph and histogram of 2.31×10^{-4} M (PdSn)–2-propanol ($t=0$). Magnification ×200,000 Mean size $\mu=5.8$ nm, $\sigma=1.5$ nm

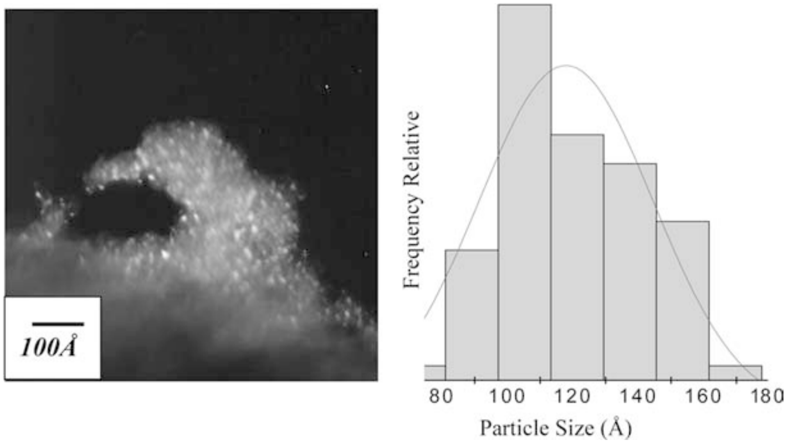

Fig. 2 Electron micrograph and histogram of $2.31{\times}10^{-4}$ M (PdSn)–2-propanol after 4 months. Magnification ×100,000. Mean size $\mu = 10.0$ nm, $\sigma = 2.2$ nm

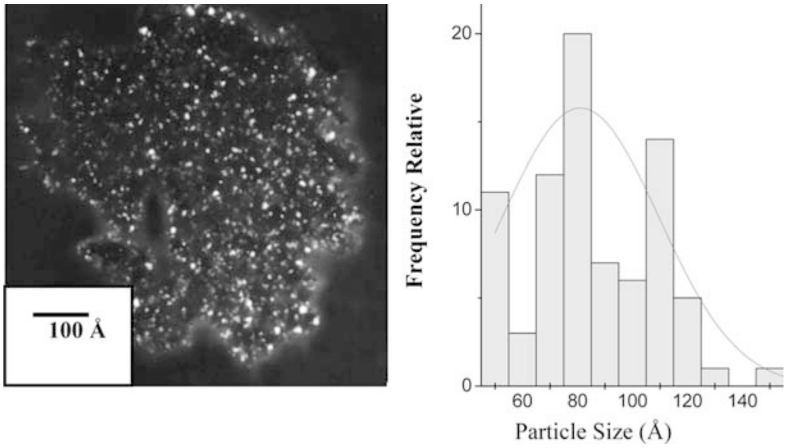

Fig. 3 Electron micrograph and histogram of $2.29{\times}10^{-4}$ M (PdSn)–acetone (t = 0). Magnification ×100,000. Mean size $\mu = 8.3$ nm, $\sigma = 2.2$ nm

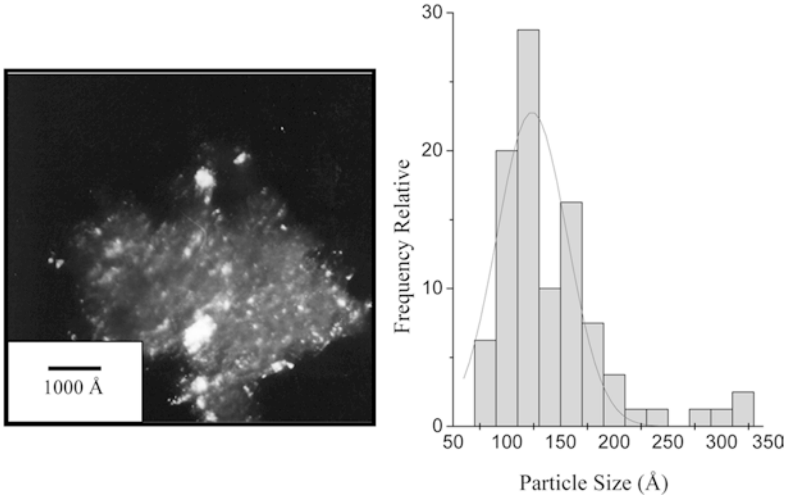

Fig. 4 Electron micrograph and histogram of $2.29{\times}10^{-4}$ M (PdSn)–acetone after 7 months. Magnification ×100,000. Mean size $\mu = 12.0$ nm, $\sigma = 5.0$ nm

potential between that of both monometallic colloids: 44 mV for Pd [21] and 1,076 mV for Sn [22], respectively. This phenomenon was observed previously for Ni–Cu colloids [23]. See Table 1.

Electron micrograph of the colloids were obtained to find out the shapes and sizes. The sizes of the particles are represented in a histogram and the standard deviation was calculated. Figures 1, 2, 3, 4, 5 and 6 show the

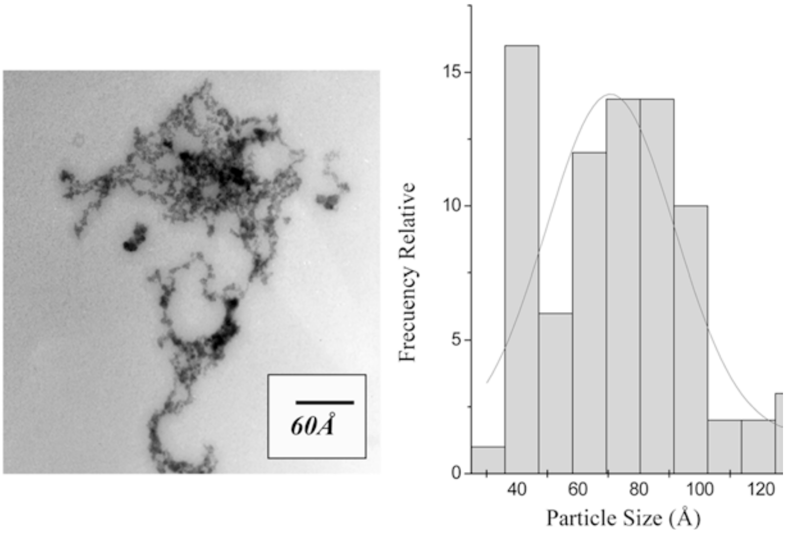

Fig. 5 Electron micrograph and histogram of 2.29×10^{-4} M (PdSn)–ethanol (t =0). Magnification ×60,000. Mean size $\mu = 7.0$ nm, $\sigma = 2.3$ nm

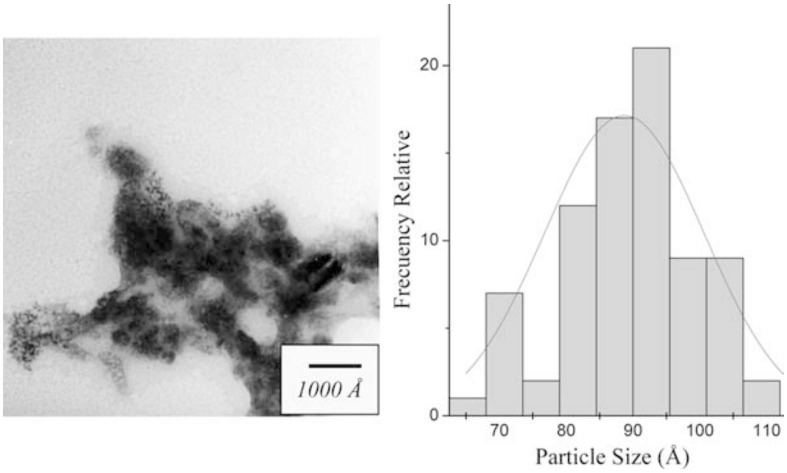

Fig. 6 Electron micrograph and histogram of 2.29×10^{-4} M (PdSn)–ethanol after five months. Magnification ×100,000. Mean size $\mu = 9.0$ nm, $\sigma = 1.1$ nm

Table 2 Particle size aging of Pd–Sn colloids

Solvent	Concentration (mol l^{-1}×10^{-3})	Time (months)	Particle size (nm)
2-Propanol	0.231	0	5.80
		4	10.00
Acetone	0.228	0	8.30
		7	12.35
Ethanol	0.229	0	7.00
		5	8.87

electron micrographs of the PdSn colloids. Most of the colloid exhibited one distribution of particle size, which means that most of the particles are bimetallic. The electron micrograph for (PdSn)–2-methoxyethanol colloid at zero time shows the presence of metal clusters dispersed in the metal grid with a particle size of 3.8 nm.

(PdSn)–acetone colloids show a particle size of 12.35 nm; after 7 months at room temperature the size increases owing to clustering (Fig. 4). A narrowing distribution is observed. (PdSn)–ethanol colloids exhibit a particle size of 8.87 nm; after 5 months at room temperature the size remains almost the same (Fig. 6). However, in the case of 2-propanol the PdSn colloid increases in size from 5.8 to 10 nm, mainly owing to the higher viscosity (Figs. 1, 2). These colloids show similar stability to Au–2-propanol colloids, which are also spherical and negatively charged particles [23]. The narrow particle size distribution becomes wider with aging of the colloid. The values are summarized in Table 2. Also, bimetallic–2-propanol colloids just prepared exhibit a particle size of 5.1 nm [24], which is very similar to that (PdSn)–2-propanol.

The PdSn colloids exhibit a UV absorption ranging from 200 to 306 nm which is in the range of theoretical values found for Sn (210 nm) and Pd (250 nm), respectively [25]. The PdSn–2-butanone colloid exhibits a λ_{max} of 309 nm and PdSn–2-propanol shows a λ_{max} of 292 nm. The other absorption of PdSn–acetone is at $\lambda_{max} = 210$ nm. This difference in absorption is most probably due to the different particle size of the colloids. (Table 3). After solvent evaporation under vacuum powders and active solids were obtained.

A complete study by IR spectroscopy was carried out for solvents and films. Let us consider PdSn–acetone that shows a band corresponding to $\nu_{C=O}$ at 1,588 cm^{-1} (Table 4)· This is indicative of a metal–solvent interaction with a structure probably of a four-metal center involving both metals.

PdSn–2-methoxyethanol exhibits bands corresponding to $\nu_{C\text{-}O}$ at 1,260 and 1,094 $cm^{-1,}$ showing the presence of the solid.

Table 3 UV absorption of Pd–Sn bimetal colloids

Solvent	Colloid concentration ($M \times 10^{-3}$)	$\lambda_{max.}$ (nm)
2-Propanol	2.24	292
Ethanol	2.33	200
2-Methoxyethanol	2.32	205
Acetone	2.36	210
2-Butanone	2.28	306

A TGA-FTIR study was carried out with the Pd–Sn solids. It is interesting to observe the presence of acetone in the films (Table 5); $\nu_{C=O}$ at 1,704 cm^{-1} can be observed. The presence of 2-methoxyethanol was also observed in the films. The presence of characteristic bands is evidence of carbonaceous material inside the metal clusters of Pd and Sn.

During the heating of the (PdSn)–2-methoxyethanol solid the decomposition produces ethylene and acetone catalyzed by Sn. This observation is corroborated by the presence of $\nu_{C=C}$ at 1,692 cm^{-1} and $\nu_{C=O}$ at 1745 cm^{-1}, respectively (Table 5).

Conclusions

It was possible to obtain stable bimetallic Pd–Sn colloids and also to determine their particle size. During the aging at room temperature ethanol colloids remain as sols with similar particle size. On using 2-propanol the colloids double in size owing to the higher viscosity.

The work conditions, such as the amount of the metals, speed of solvent addition and warm up speed, can be controlled to obtain different particle sizes.

Table 4 Fourier transform IR absorption of Pd–Sn solids

Solids	Band	Wavenumber (cm^{-1})
(PdSn)–2-propanol	ν_{-OH}	3,414
	ν_{C-O}	1,394, 1,056 (alcohol 2°)
(PdSn)–2-methoxyethanol	ν_{-OH}	3,430
	ν_{-OCH3}	2,963
	ν_{C-O}	1,260, 1,094–1027 (alcohol 1°)
(PdSn)–ethanol	ν_{OH}	3,392
	ν_{-CH3}	2,934
	ν_{C-O}	1,263–1,051 (alcohol 1°)
(PdSn)–2-butanone	$\nu_{C=O}$	1,620
	ν_{CH3-CO}	1,382
	ν_{CH3}	2,973
(PdSn)–acetone	ν_{C-O}	1089 and 1024, 1,588 [a]
	ν_{-CH3}	2,965
Sn–acetone	$\nu_{C=O}$	1,625
	ν_{CH3-CO}	1,383

[a] For acetone solids, the disappearance of the C = O bond is due to a four-center bridge being established with the metals

Table 5 Thermal behavior of Pd–Sn solids and thermogravimetric analysis (*TGA*)-Fourier transform (*FT*) IR spectroscopy results

Solids	T_D	Weight loss (%)	TGA-FTIR	
			Band	Wavenumber (cm^{-1})
(PdSn)–propanol	–	–	ν_{OH}	3,734
			$\nu_{C-(CH3)2}$	1,450
(PdSn)–ethanol	53.78, 325.35	37.15	ν_{OH}	3,741
			ν_{C-CH3}	1,513
(PdSn)–2-methoxyethanol	222, 247	9.27	ν_{OH}	3,741
			$\nu_{C=C}$	1,692
			$\nu_{C=O}$	1,745
(PdSn)–acetone	412	12.96	$\nu_{C=O}$	1,704
			ν_{CH3-CO}	1,360
			ν_{CH3}	1,450

The amorphous films exhibit the presence of the solvent in the metal clusters from the decomposition studies of the films.

Acknowledgement The authors thank Fondecyt, grant 1000527, and the Dirección de Investigación of the Universidad de Concepción for financial support.

References

1. Klabunde KJ (1989) Chemistry of free atoms and particles. Academic Press, New York
2. Cárdenas G, Klabunde KJ, Dale EB (1987) Langmuir 3:986
3. Cárdenas G, Klabunde KJ, Dale EB (1987) Proc Opt Eng SPIE 821:206
4. Cárdenas G, Klabunde KJ (1988) Bol Soc Chil Quím 33:163–175
5. Cárdenas G, Alvial M, Klabunde KJ, Xi LY (1992) Bol Soc Chil Quím 37 > 19–25
6. Riecke RD (1975) Top Curr Chem 59:1
7. Burns TP, Riecke RD (1987) J Org Chem 52:3674
8. Klabunde KJ, Cárdenas-Triviño G (1996) Metal atom/vapor approaches to active metal clusters/particles. VCH, New York, pp 237–278
9. Eastman J, Siegel RW (1989) In: Eastman J, Siegel RW (eds) Nanophase synthesis assembles materials from atomic clusters. p 56
10. Siegel RW (1994) Nanostruct Mater 4:121
11. Gleiter H (1995) Mater Sci Forum 67:189
12. Cárdenas G, Vera V, Muñoz C (1988) Mater Res Bull 33:645
13. Cárdenas G, Segura R, Morales J, Soto H, Lima CA (2000) Polyhedron 19:2337
14. Cárdenas G, Acuña J (2001) Colloid Polym Sci 279:442
15. Reisfled R (1966) Structure and bonding, vol 85. Springer, Berlin Heidelberg New York
16. Beecroft LL, Ober CK (1997) Chem Mater 9:1302
17. Banyai L, Hu YZ, Lindberg M, Koch SW (1988) Phys Rev B 38:8142
18. Cárdenas G, Ponce A (1996) Colloid Polym Sci 274:788
19. Cárdenas G, Alvial M, Klabunde KJ (1990) Bol Soc Chil Quím 35:277
20. Cárdenas G, Segura R (2000) Mater Res Bull 35:1369
21. Cárdenas G, Muñoz C, Vera V (1996) Bol Soc Chil Quím 41:235
22. Cárdenas G, Alvial M (1994) Colloid Polym Sci 272:310
23. Cárdenas G, Oliva R (1998) Mater Res Bull 33:1599
24. Cárdenas G, Vera V, Gónzalez V, Navarro M (1997) Mater Res Bull 32:97–106
25. Creighton JA, Eadon DG (1991) J Chem Soc Faraday Trans 87:3881–3891